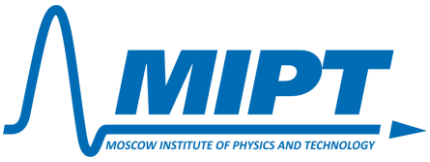

Recent Developments in Soft X-Ray Pulse Shaping

Summer student: Roman Kamyshinskii [1,2,4],

Supervisors: Leslie Lamberto Lazzarino [3], Sergey Usenko [4]

[1] *Moscow Institute of Physics and Technology (State University), Dolgoprudny, Moscow Region, Russian Federation*

[2] *National Research Centre "Kurchatov Institute", Moscow, Russian Federation*

[3] *University of Hamburg, Germany*

[4] *Deutsches Elektronen-Synchrotron (DESY), Hamburg, Germany*

September 7, 2017

Abstract

Pulse shaping is a way to control the spectral phase, polarization or amplitude of laser pulse. Being around for more than 40 years, this method has been used mostly in range of visible light, UV and near infrared, proving its efficiency in diverse applications. Today's technologies allow us to look above the usual pulse shaping implementation, widening it in the direction of soft X-rays and XUV. Usage of the pulse shapers in this new wavelengths range will drastically increase experimental opportunities such as coherent control studies on molecules and atoms. 4-f geometry of the device will provide the ultimate time resolution to change an outcome pulse.

In this report we will give a brief overview on pulse shaping techniques and on the device that has been built. We will focus particularly on the pulse shaper alignment and commissioning.

Contents

1. Introduction

1.1. Pulse shapers: from visible to XUV

Since the invention of lasers in 1960 there has always been a huge interest in generation and characterization of ultrashort picosecond (10^{-12} s) and femtosecond (10^{-15} s) laser pulses. Such pulses can be used in various fields of research, such as biological imaging [1], optical communications [2], coherent control [3] and multidimensional spectroscopy [4].

The shape of the pulse can be defined by its complex electric field in the spectral or time domain. Both spectral amplitude and phase contribute to the pulse shape [5].

There are two fundamentally different approaches on pulse shaping. One of them uses a closed loop scheme, when outcomes of different shapes are returned into an iterative algorithm that optimizes the excitation shape. On the other hand, there is an open loop scheme that is mostly used concerning small systems with reliable theoretical predictions. This approach suggests that temporal response of a system excited by a light pulse can be manipulated without any experimental response due to theoretical predetermination.

Pulse shaping techniques, based on time-invariant filter can be portrayed either in the time domain or in the frequency domain. The output of linear filter is actually a convolution of the impulse response of the pulse shaper with the input signal. For devices which operate in spectral domain the output pulse is equal to transfer function (which describes the pulse shaper) multiplied by input pulse.

Pulse shapers built on programmable mask have a huge variety of applications, as they address spectral components of the pulse by spatial separation, introducing a spatiotemporal coupling. The main other devices for pulse shaping, less versatile than programmable masks, are shown in Fig. 1.

Scheme of set-up	Transfer function
(a) 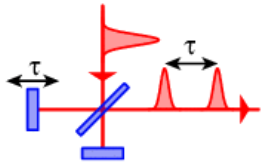	$H(\omega) = \frac{1}{2}(1 + e^{i\omega\tau})$
(b) 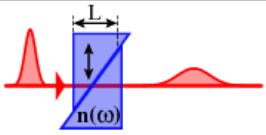	$H(\omega) = e^{i\phi(\omega)}$ $\phi(\omega) = n(\omega) L\omega/c$
(c) 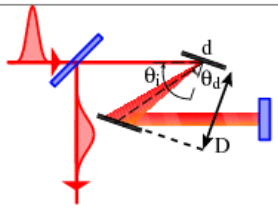	$H(\omega) = e^{i\phi(\omega)}$ $\phi(\omega) = 2\frac{\omega}{c} D \frac{\cos(\theta_i + \theta_d)}{\cos\theta_i}$
(d) 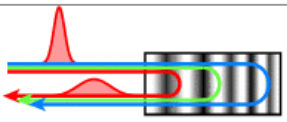	$H(\omega) = \lvert H(\omega)\rvert e^{i\phi(\omega)}$ $\lvert H(\omega)\rvert$ is the reflectivity $\phi(\omega)$ designed until the fourth order

Figure 1. *Simple shaping set-ups. (a) Michelson interferometer producing two delayed pulses, (b) propagation through a dispersive bulk medium (length L, index n), (c) grating compressor (θ_i incident angle, θ_d diffraction angle, D distance between the two gratings and d the interline spacing) and (d) chirped mirror (the penetration depth depends on the wavelength which introduces chirp on a Fourier-limited pulse). Adapted from [5].*

1.2. Pulse Shaping in 4f – geometry

4f-line (or zero dispersion line) is a spectrometer composed of 4 optical components separated from each other by a distance f, which is the focal length of the mirror, therefore all the spectral components are focused in the Fourier plane in the middle of the device [6]. Input wavelengths are angularly dispersed by the first grating, and then are focused by the first mirror to diffraction spots in the Fourier plane. The second mirror and grating, identical to the first ones, allow the recombination of all the spectral components into a single beam. The output pulse shape is identical to the input one, unless a mask is placed in the Fourier plane (FP) (Fig. 2).

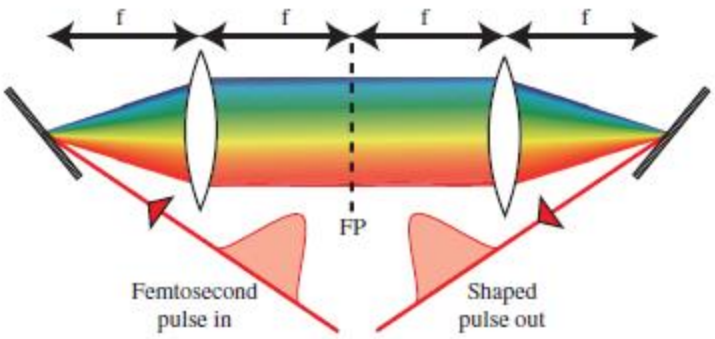

Figure 2. *A 4f setup: dispersion line composed of two gratings and two mirrors of focal length f. The output pulse is identical to the input pulse. Adapted from [5]*

Depending on the mask it is possible to control the polarization [9], the phase [10] or both phase and amplitude [11] of a 4f pulse shaper.

1.3. Basic equations for 4f - geometry

The input pulse is considered to be Gaussian in time and space with a central wavelength λ_0, corresponding to a central frequency ω_0, and the FWHM intensity is Δx_{in} in in the spatial domain, Δt in the temporal domain and ω_L in the spectral domain [7].

The input pulse is coming with an angle θ_i and gets diffracted with an angle θ_d at λ_0 by the 1st grating with the period d. The focal length of the mirror is f (Fig.3). As a result of diffraction each spectral component in the Fourier plane has a limited size Δx_0, which can be determined using Gaussian beam propagation: $\Delta x_0 = 2ln(2)f\lambda_0 cos\theta_i/\pi\Delta x cos\theta_d$

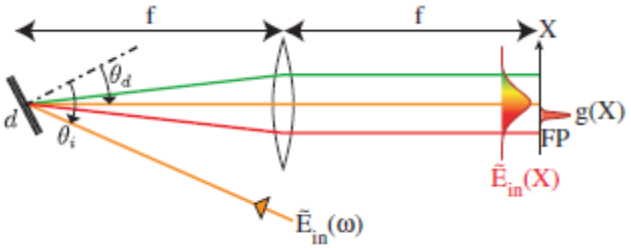

Figure 3. *Half a 4-f line*

In case of linear dispersion, a frequency ω_k is located in the Fourier plane at X_k given by

$$X_k = \alpha\omega_k$$

where $\alpha = \lambda_0^2 f / 2\pi cdcos\theta_d$ is set by the $4f$ -line geometry and X_k is spatial coordinate. Through the Fourier transform the frequency resolution

$$\delta\omega = \frac{\Delta x_0}{\alpha}$$

corresponds to a window

$$T = \frac{4\ln(2)}{\delta\omega} = \frac{\Delta x_{in}}{|v|}$$

in the time domain, where

$$v = \frac{cd\cos\theta_i}{\lambda_0}$$

and has the dimension of velocity. T defines the time window available for shaping and it is proportional to the input waist, as the equation states. This property of the $4f$ -line points to spatiotemporal coupling. T defines the maximum duration or the time delay for shaping achievable with such a $4f$ -line.

With a mask in the Fourier plane a $4f$ -line becomes a pulse shaper. In order to maximize pulse shaping capability the subsequent condition should be fulfilled:

$$control\ parameter\ number\ \geq\ \Delta\eta$$

Where $\eta = \Delta\omega/\delta\omega$ is the complexity [10] (fig 4).

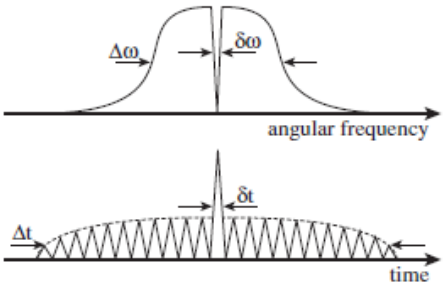

Figure 4. *The complexity can be seen as the ratio between the largest and smallest features in either spectral or time domain. Adapted from [5].*

The mask will act both as a spectral mask M_ω and a spatial mask M_X. Immediately after the mask, the pulse can be written as

$$\tilde{E}_{after}(\omega, X) = \tilde{E}_{in}(\omega) \cdot g(X - \alpha\omega) M_X(X)$$

where

$$g(X) = \exp\left[-2\ln(2)\left(\frac{X}{\Delta x_0}\right)^2\right]$$

is the spatial extension of a given frequency component. As the position and frequency are coupled in the Fourier plane, both the spectral and spatial components of the pulse are affected by the mask. Assuming that the spatial profile is unaffected by the mask, Gaussian propagation gives a linear expression for the output pulse

$$\tilde{E}_{out}(\omega) = H(\omega)\tilde{E}_{in}(\omega)$$

where $H(\omega) = M_{\omega'} g(\omega' - \omega)d\omega' = M_\omega \otimes g(\omega)$ and $M_\omega(\omega) = M_X(\alpha\omega)$.

This expression is only valid for simple shapes and for the on-axis part of the pulse.

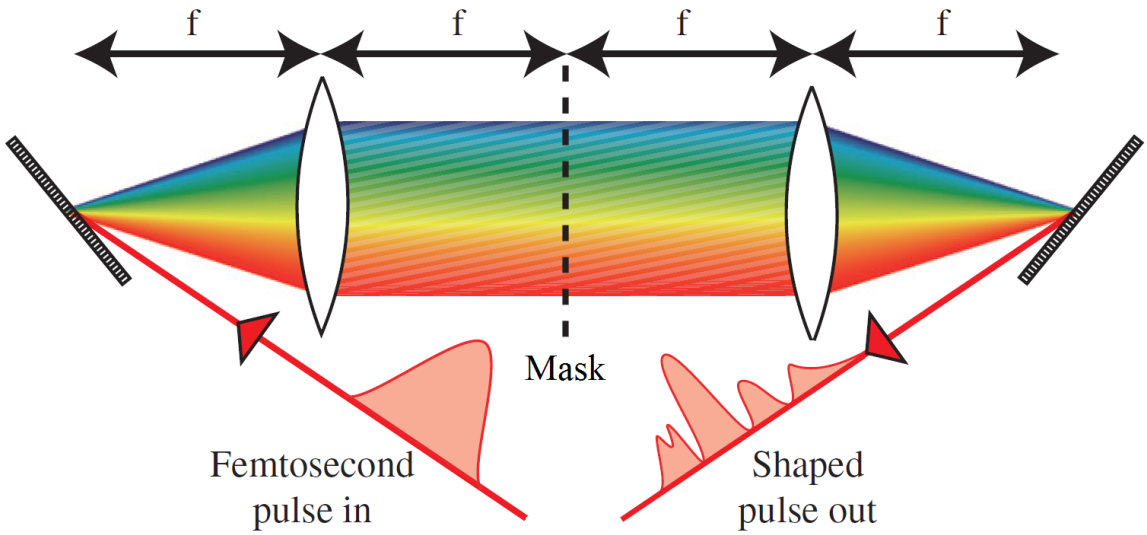

Figure 5. *Pulse shaper based on a use of 4f-line with a mask in a Fourier plane. Adapted from [5].*

1.4. sFLASH

sFLASH is an experiment for studying seeding schemes for free-electron laser (FEL) facility FLASH at DESY. A seeding scheme is a way to generate temporally coherent FEL radiation either by manipulating the internal structure of the electron bunch by external lasers or using an external light field as a direct seed for the FEL amplifier.

Free-electron lasers (FEL) produce fully coherent radiation in the extreme ultra-violet (XUV), soft, and hard X-ray spectral range, which is highly demanded for a huge variety of scientific experiments. For a long time FELs were operated using the principle of self-amplified spontaneous emission (SASE) [13]. Nonetheless, due to the nature of the way in which this spontaneous amplification occurs, such pulses lack temporal coherence. In contrast to that, an external seed source which initiates the FEL process allows to maintain the temporal coherence of the seed, therefore improving the temporal and energy resolution of FEL experiments [8]. The FLASH seeding experiment sFLASH uses its own undulators (Fig. 6) in the accelerator tunnel for this purpose, as well as a special measuring station in the FLASH tunnel, at which the pulses of photons can be examined.

Figure 4 shows a schematic layout of the FLASH1 FEL beamline. After the energy collimator, the seeding section starts with two short electro-magnetic undulators (MOD1 and MOD2) each

followed by a magnetic chicane C1 and C2. Four variable-gap undulators act as the FEL radiators. The FEL pulses are guided to a photon diagnostics section using a mirror system. The chicane C3 steers the electron beam around the extraction mirrors. The following dispersive dump section and a transverse deflecting structure allows to diagnose the longitudinal phase space distribution of the electron bunches.

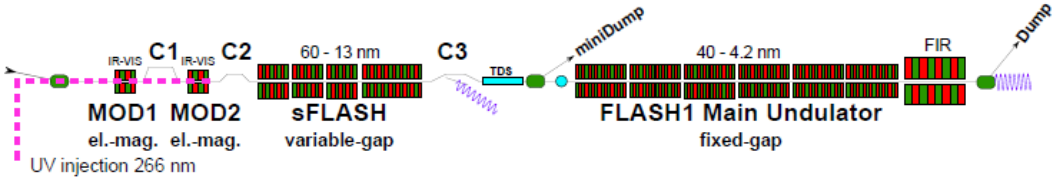

Figure 6. *Layout of the FLASH1 beamline. Adapted from [8]. An overview of the entire FLASH facility can be found in [12]*

The seeding experiment at FLASH was conducted using the HGHG (High-Gain Harmonic Generation) procedure. The laser light was superimposed with a wavelength of 266 nm on an electron beam from FLASH. During its trajectory through the undulator, the packet of electrons is divided into a periodic microstructure, which leads to a selective amplification of the FEL radiation. At 38.1 nm the seventh harmonic of 266nm, they managed to produce high-intensity flashes of FEL light with an energy of over 100 µJ in the sFLASH undulator. This result marked a crucial step towards studying an as yet unknown area of FEL seeding technology. At the same time, it shows that this principle perfectly augments the unique properties of the electron beam at FLASH, to create fully coherent, i.e. laser-like, pulses of radiation in the extreme ultraviolet range of the spectrum.

2. Outline of experiment

2.1. Experimental setup

The layout of experimental setup is shown schematically in Fig. 7. It consists of 5 vacuum chambers, connected to each other, and details inside them which will be discussed further.

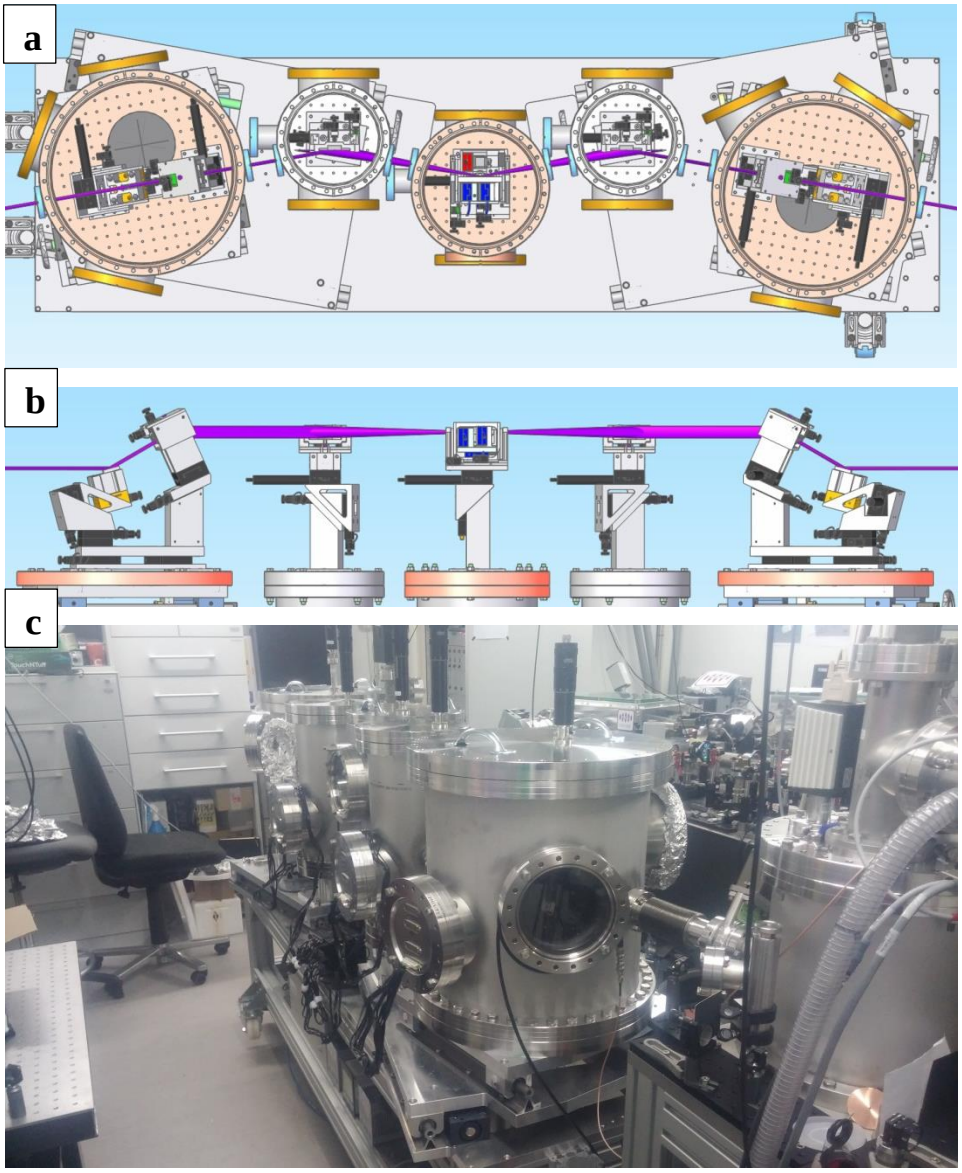

Figure 7. *Top view (a) and side view (b) layouts of experimental setup (adapted from[]), and a final picture of the pulse shaper(c)[].*

To obtain a well-focused beam it is necessary to align all the moving parts inside of the vacuum chambers of pulse shaper. Therefore, after building the mainframe of the device and making all the necessary details, the initial step was to mount picomotors for all the moving parts of the pulse shaper, such as gratings, mirrors and mask to make it possible to properly align the system. In order to avoid any inconveniences in the future, a labelling list for picomotors and switches in which they are plugged was made.

A 635 nm alignment laser and a system of screens was used for the alignment of the device (Fig. 8). Screens were covered with Ce:YAG powder to allow alignment of XUV and soft x-rays.

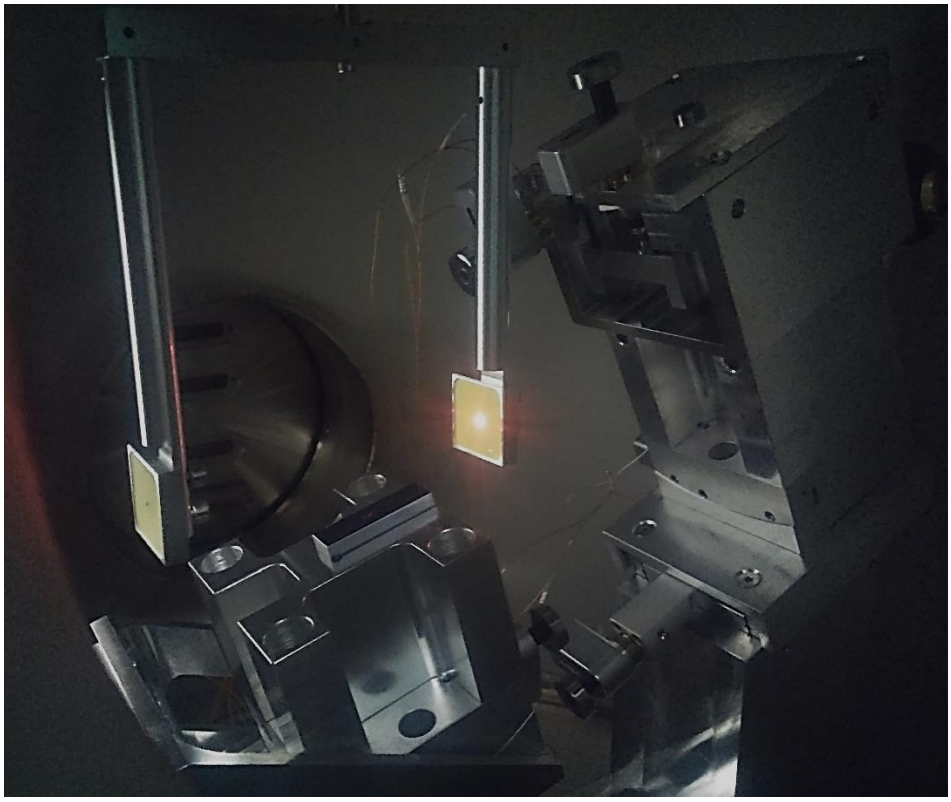

Figure 8. *A picture of 400 nm laser beam reflected from the mirror to the removable alignment screen mounted in a chamber.*

The phase mask allows modification of the relative phase of different wavelength (Fig. 9). The mask is formed by two striped interleaved flat mirrors, which allows creation of two copies of input pulse with variable delay. Thus, the input laser spectrum is viewed as a superposition of independent but interlaced combs assigned to different sub-pulses.

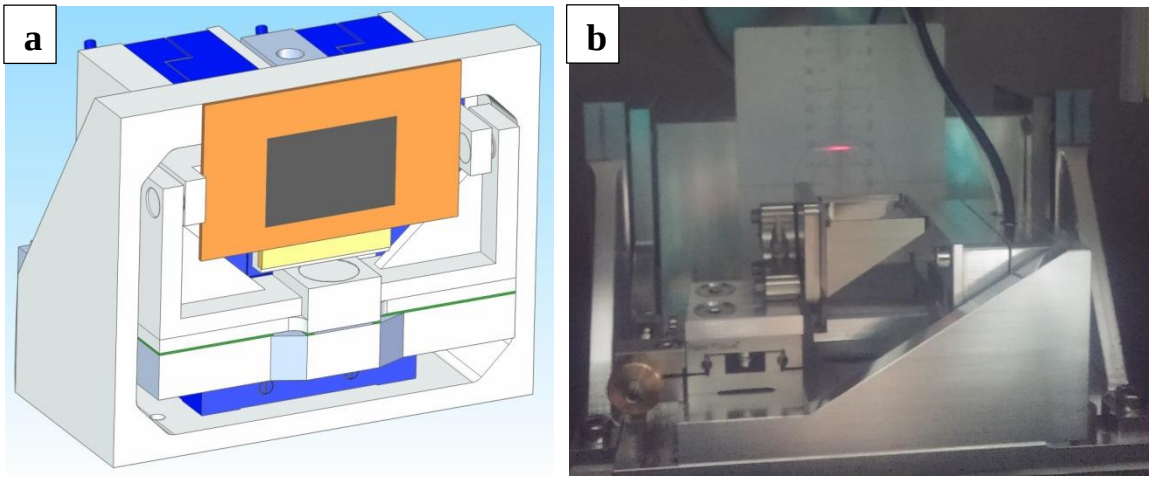

Figure 9. *A scheme of comb mask mount (a) and line of 400 nm alignment laser on the Fourier plane(b).*

2.2. Spectroscopy

To commission the laser/electron overlap 266 nm seed pulses are generated by third-harmonic generation (THG) of near-infrared (NIR) Ti:sapphire laser pulses. The final goal will be to obtain spectra from the seeding experiment in high-gain harmonic generation (HGHG) mode with a seed wavelength of 266 nm (and lasing at the 7^{th}, 8^{th}, and 9^{th} harmonic).

The SPM002 Spectrometer (Photon Control, Canada) was tested for use for the pulse shaper alignment as well as for UV spectrum measurement before and after the pulse shaping. Wide spectral range of the spectrometer provided an opportunity to study 800 nm, 400 nm and 266 nm pulses. SPECSOFT software (Photon Control, Canada) was used for data collection and spectroscopic measurements.

The IR laser spectrum was expected to be 800 nm. However, after the measurement a peak with a wavelength close to 787 nm was indicated (Fig. 10). Such a deviation will need investigation, and could partially explain the low tripler performances witnessed (only 12% conversion to the second harmonic, instead of 25% claimed by the company selling it, under 1% conversion to the third harmonic, instead of 8% claimed).

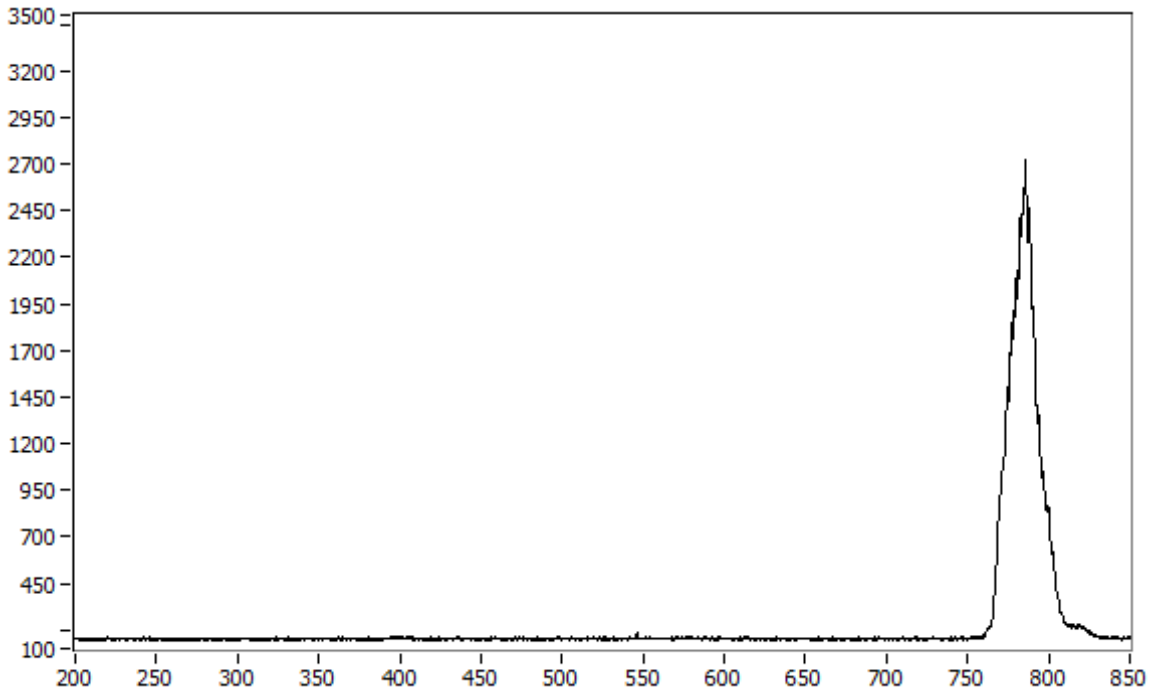

Figure 10. *A spectrum of 800 nm laser pulse. FWHM = 18 nm*

A 400 nm peak (Fig. 11) appears to be 397 nm with FWHM of 3 nm, while a 266 nm pulse is centred at 266nm as expected (Fig. 12) with FWHM of 2.8 nm.

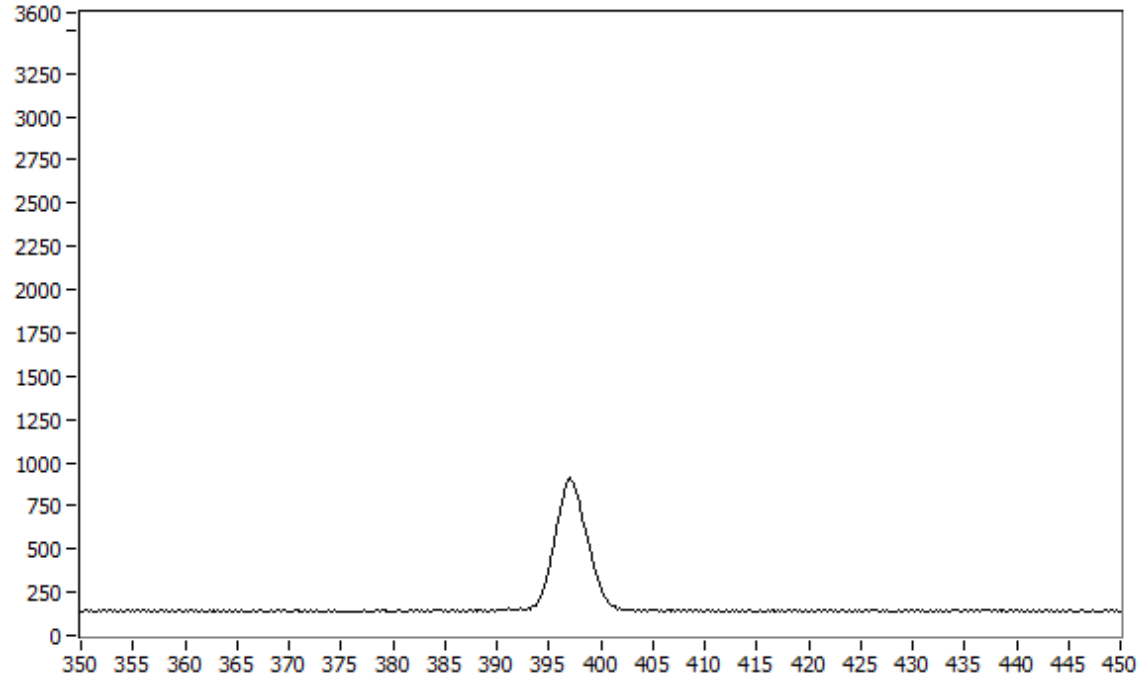

Figure 11. *A spectrum of 400 nm laser pulse. FWHM = 3 nm.*

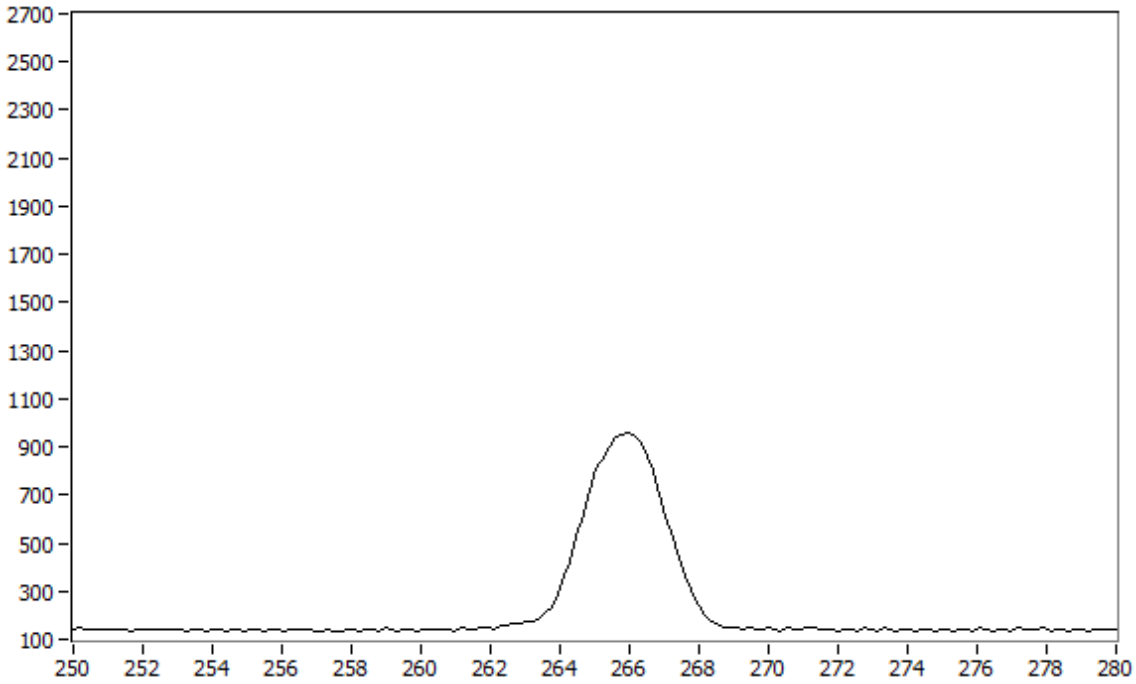

Figure 12. *A spectrum of 266 nm laser pulse. FWHM = 2.8 nm.*

3. Conclusion

Unfortunately, at this moment a few things still need to be improved: the tripler power output at 266nm is too low for measurements and pulse shaping (Fig. 13). The latest attempt at increasing the power resulted in a good improvement over the previous situation, as can be seen comparing Fig. 13 with Fig. 14. Although we achieved a lot over such a short amount of time, there are still a few things that need to be taken care of before conducting the first 266nm experiment, and a few more before the final XUV pulse shaping experiment.

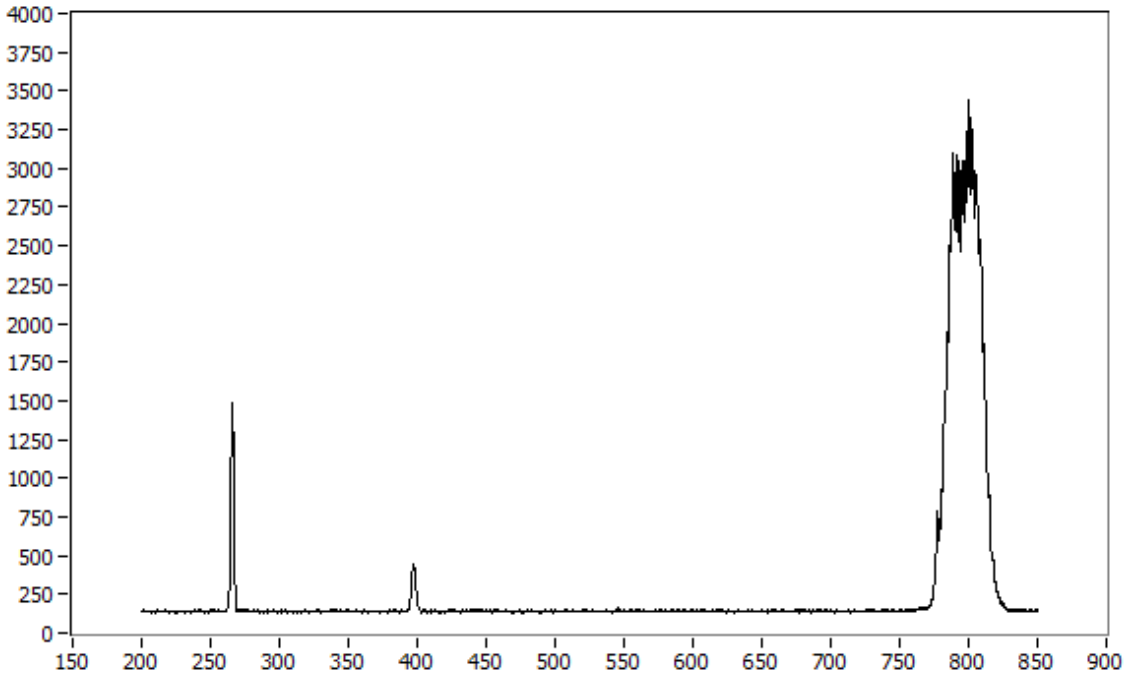

Figure 13. *Spectra of 266, 400 and 800 nm laser pulses.*

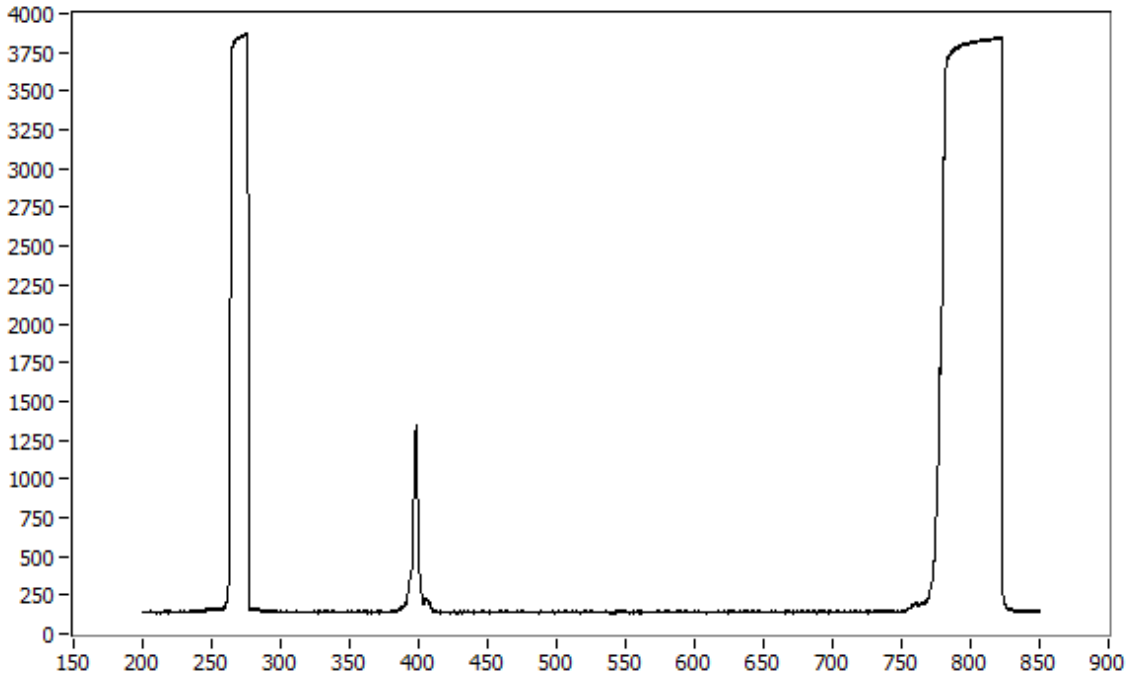

Figure 14. *Spectra of 266, 400 and 800 nm laser pulses with increased power.*

References

1. Silberberg Y 2009 Quantum coherent control for nonlinear spectroscopy and microscopy Annu. Rev. Phys. Chem. 60 277–92

2. Sardesai H P, Chang C C and Weiner A M 1998 A femtosecond code division multiple-access communication system test bed J. Lightwave Technol. 16 1953

3. Dantus M and Lozovoy V V 2004 Experimental coherent laser control of physicochemical processes Chem. Rev. 104 1813–59

4. Shim S-H and Zanni M T 2009 How to turn your pump-probe instrument into a multidimensional spectrometer: 2D IR and VIS spectroscopies via pulse shaping Phys. Chem. Chem. Phys. 11 748–61

5. Monmayrant A, Weber S and Chatel B Newcomer's guide to ultrashort pulse shaping and characterization J.of Phys. B: At. Mol. Opt. Phys. 43 (2010) 103001 (34pp)

6. Froehly C, Colombeau B and Vampouille M 1983 Shaping and analysis of picosecond light pulses *Prog. opt.* **20** 65–153

7. Danailov M B and Christov I P 1989 Time-space shaping of light pulses by fourier optical processing J. Mod. Opt.
36 725–31

8. Bödewadt J., Laarmann T., Lazzarino L. et al. Recent results from FEL seeding at FLASH Proceedings of IPAC2015, Richmond, VA, USA 2015

9. Brixner T and Gerber G 2001 Femtosecond polarization pulse shaping Opt. Lett. 26 557–9

10. Weiner A M 2000 Femtosecond pulse shaping using spatial light modulators Rev. Sci. Instrum. 71 1929–60

11. Weiner A M, Heritage J P and Kirschner E M 1988 High-resolution femtosecond pulse shaping J. Opt. Soc. Am. 5 1563–72

12. M. Vogt et al.., "Status of the Soft X-ray Free Electron Laser FLASH", TUPWA033, These Proceedings, IPAC'15, Richmond, VA, USA (2015).

13. A. M. Kondratenko and E. L. Saldin, Part. Accel. 10, 207 (1980).